Chapter 6

Modified Gravity Theories: Distinguishing from ΛCDM Model

Koichi Hirano

Additional information is available at the end of the chapter

http://dx.doi.org/10.5772/intechopen.68281

Abstract

The method and probability of distinguishing between the Λ cold dark matter (ΛCDM) model and modified gravity are studied from future observations for the growth rate of cosmic structure (Euclid redshift survey). We compare the mock observational data to the theoretical cosmic growth rate by modified gravity models, including the extended Dvali–Gabadadze–Porrati (DGP) model, kinetic gravity braiding model, and Galileon model. In the original DGP model, the growth rate $f\sigma_8$ is suppressed in comparison with that in the ΛCDM model in the setting of the same value of the today's energy density of matter $\Omega_{m,0}$, due to suppression of the effective gravitational constant. In the case of the kinetic gravity braiding model and the Galileon model, the growth rate $f\sigma_8$ is enhanced in comparison with the ΛCDM model in the same value of $\Omega_{m,0}$, due to enhancement of the effective gravitational constant. For the cosmic growth rate data from the future observation (Euclid), the compatible value of $\Omega_{m,0}$ differs according to the model. Furthermore, $\Omega_{m,0}$ can be stringently constrained. Thus, we find the ΛCDM model is distinguishable from modified gravity by combining the growth rate data of Euclid with other observations.

Keywords: accelerated expansion, gravitational theory, dark energy, observational test, cosmic growth rate

1. Introduction

Cosmological observations, including type Ia supernovae (SNIa) [1, 2], cosmic microwave background (CMB) anisotropies, and baryon acoustic oscillations (BAO), indicate that the universe is undergoing an accelerated phase of expansion. This late-time acceleration is one of the biggest mysteries in current cosmology. The standard explanation is that this acceleration is

caused by dark energy [3–6]. This would mean that a large part of components in the universe is unknown. The cosmological constant is a candidate of dark energy. To explain the late-time accelerated expansion of the universe, the cosmological constant must be a very small value. However, its value is not compatible with a prediction from particle physics, and it has fine-tuning and coincidence problems.

An alternative explanation for the current acceleration of the universe is to modify general relativity to be a more general theory of gravity at a long-distance scale. Several modified gravity theories have been studied, such as $f(R)$ gravity (for reviews, see, e.g., [7]), scalar-tensor theories [8–10], and the Dvali–Gabadadze–Porrati (DGP) braneworld model [11–13].

Furthermore, as an alternative to general relativity, Galileon gravity models have been proposed [14–22]. These models are built by introducing a scalar field with a self-interaction whose Lagrangian, which is invariant under Galileon symmetry $\partial_\mu\phi \to \partial_\mu\phi + b_\mu$, keeps the field equation of motion as a second-order differential equation. This avoids presenting a new degree of freedom, and perturbation of the theory is free from ghost or instability problems. The simplest term of the self-interaction is $\Box\phi(\nabla\phi)^2$, which induces decoupling of the Galileon field from gravity at small scales via the Vainshtein mechanism [23]. Therefore, the Galileon theory recovers general relativity at scales around the high-density region, as is not inconsistent with solar system experiments.

Galileon theory has been covariantized and studied in curved backgrounds [24, 25]. Although Galileon symmetry cannot be maintained in the case that the theory is covariantized, it is possible to preserve the equation of motion at second order, which means that the theory does not raise ghost-like instabilities. Galileon gravity induces self-accelerated expansion of the current universe. Thus, inflation models inspired by the Galileon gravity theory have been studied [26–28]. In Ref. [29], the parameters of the generalized Galileon cosmology were constrained from the observational data of SNIa, CMB, and BAO. The evolution of matter density perturbations for Galileon cosmology has also been investigated [16–18, 30, 31].

Almost 40 years ago, Horndeski derived the action of most general scalar-tensor theories with second-order equations of motion [32]. His theory received much attention as an extension of covariant Galileons [14, 24, 25, 33]. One can show that the four-dimensional action of generalized Galileons derived by Deffayet et al. [34] is equivalent to Horndeski's action under field redefinition [35]. Because Horndeski's theory contains all modified gravity models and single-field inflation models with one scalar degree of freedom as specific cases, considerable attention has been paid to various aspects of Horndeski's theory and its importance in cosmology.

Recently, more general modified gravity theories have been studied, including Gleyzes-Langlois-Piazza-Vernizzi (GLPV) theories [36, 37] and eXtended Galileon with 3-space covariance (XG3) [38].

In this chapter, the probability of distinguishing between the Λ cold dark matter (ΛCDM) model and modified gravity is studied by using future observations for the growth rate of cosmic structure (e.g., Euclid redshift survey [39]). We computed the growth rate of matter density perturbations in modified gravity and compared it with mock observational data. Whereas the background expansion history in modified gravity is almost identical to that of dark energy

models, the evolution of matter density perturbations of modified gravity is different from that of dark energy models. Thus, it is important to study the growth history of perturbations to distinguish modified gravity from models based on the cosmological constant or dark energy.

Although past observations of the growth rate of matter density perturbations have been used to study modified gravity [40], we focus on future observations of the growth rate by Euclid. We adopt the extended DGP model [41], kinetic gravity braiding model [30], and Galileon model [16, 17] as modified gravity models. The kinetic gravity braiding model and the Galileon model are specific aspects of Horndeski's theory.

This chapter is organized as follows. In the next section, we present the background evolution and the effective gravitational constant in modified gravity models. In Section 3, we describe the theoretical computations and the mock observational data of the growth rate of matter density perturbations. In Section 4, we study the probability of distinguishing between the ΛCDM model and modified gravity by comparing the predicted cosmic growth rate by models to the mock observational data. Finally, conclusions are given in Section 5.

2. Modified gravity models

2.1. Extended DGP model

In the DGP model [11], it is assumed that we live on a 4D brane embedded in a 5D Minkowski bulk. Matter is trapped on the 4D brane, and only gravity experiences the 5D Minkowski bulk.

The action is

$$S = \frac{1}{16\pi} M_{(5)}^3 \int_{bulk} d^5x \sqrt{-g_{(5)}} R_{(5)} + \frac{1}{16\pi} M_{(4)}^2 \int_{brane} d^4x \sqrt{-g_{(4)}} (R_{(4)} + L_m), \tag{1}$$

where quantities of the 4D brane and the 5D Minkowski bulk are represented with subscripts (4) and (5), respectively. M is the Planck mass, and L_m is the Lagrangian of matter confined on the 4D brane. The transition between 4D and 5D gravity occurs at the crossover scale r_c.

$$r_c = \frac{M_{(4)}^2}{2M_{(5)}^3}. \tag{2}$$

At scales larger than r_c, gravity appears in 5D. At scales smaller than r_c, gravity is effectively bound to the brane, and 4D Newtonian dynamics is recovered to a good approximation. r_c is a parameter in this model, which has the unit of length [42].

Under spatial homogeneity and isotropy, a Friedmann-like equation is obtained on the brane [43, 44]:

$$H^2 = \frac{8\pi G}{3}\rho + \varepsilon \frac{H}{r_c}, \tag{3}$$

where ρ represents the total fluid energy density on the 4D brane. The DGP model has two

branches ($\varepsilon = \pm 1$). The choice of $\varepsilon = +1$ is called the self-accelerating branch. In this branch, the accelerated expansion of the universe is induced without dark energy, since the Hubble parameter comes close to a constant $H = 1/r_c$ as time passes. By contrast, $\varepsilon = -1$ is the normal branch. In this case, the expansion cannot accelerate without a dark energy component. Therefore, in the following, we adopt the self-accelerating branch ($\varepsilon = +1$).

The original DGP model, however, is plagued by the ghost problem [45] and is incompatible with cosmological observations [46].

Dvali and Turner [41] phenomenologically extended the Friedmann-like equation of the DGP model (Eq. (3)). This model interpolates between the original DGP model and the ΛCDM model by adding the parameter α. The modified Friedmann-like equation is

$$H^2 = \frac{8\pi G}{3}\rho + \frac{H^\alpha}{{r_c}^{2-\alpha}}. \tag{4}$$

For $\alpha = 1$, this is equivalent to the original DGP Friedmann-like equation, whereas $\alpha = 0$ leads to an expansion history identical to ΛCDM cosmology. This is important for distinguishing the ΛCDM model from the original DGP model between $\alpha = 0$ and 1. In the extended DGP model, the crossover scale r_c can be expressed as follows:

$$r_c = (1 - \Omega_{m,0})^{\frac{1}{\alpha-2}} H_0^{-1}. \tag{5}$$

Thus, the independent parameters of the cosmological model are α and today's energy density parameter of matter $\Omega_{m,0}$. The effective gravitational constant of the extended DGP model is given in order to interpolate between ΛCDM and the original DGP model. The effective gravitational constant is as follows.

$$\frac{G_{\text{eff}}}{G} = 1 + \frac{1}{3\beta}, \tag{6}$$

where

$$\beta \equiv 1 - \frac{2(r_c H)^{2-\alpha}}{\alpha}\left[1 + \frac{1}{3}\frac{(2-\alpha)\dot{H}}{H^2}\right]. \tag{7}$$

G_{eff} / G is the effective gravitational constant normalized to Newton's gravitational constant, and an overdot represents differentiation with respect to cosmic time t.

2.2. Kinetic gravity braiding model

The kinetic gravity braiding model [30] is proposed as an alternative to the dark energy model. One can say that the kinetic gravity braiding model is a specific aspect of Horndeski's theory [32].

The most general four-dimensional scalar-tensor theories keeping the field equations of motion at second order are described by the Lagrangian [32–35, 47]

$$\mathcal{L} = \sum_{i=2}^{5} \mathcal{L}_i, \tag{8}$$

where

$$\mathcal{L}_2 = K(\phi, X), \tag{9}$$

$$\mathcal{L}_3 = -G_3(\phi, X)\Box\phi, \tag{10}$$

$$\mathcal{L}_4 = G_4(\phi, X)R + G_{4,X}[(\Box\phi)^2 - (\nabla_\mu\nabla_\nu\phi)(\nabla^\mu\nabla^\nu\phi)], \tag{11}$$

$$\begin{aligned}\mathcal{L}_5 = {} & G_5(\phi, X)G_{\mu\nu}(\nabla^\mu\nabla^\nu\phi) - \frac{1}{6}G_{5,X}[(\Box\phi)^3 - 3(\Box\phi)(\nabla_\mu\nabla_\nu\phi)(\nabla^\mu\nabla^\nu\phi) \\ & + 2(\nabla^\mu\nabla_\alpha\phi)(\nabla^\alpha\nabla_\beta\phi)(\nabla^\beta\nabla_\mu\phi)].\end{aligned} \tag{12}$$

Here, K and G_i (i = 3, 4, 5) are functions of the scalar field ϕ and its kinetic energy $X = -\partial^\mu\phi\partial_\mu\phi/2$ with the partial derivatives $G_{i,X} \equiv \partial G_i/\partial X$. R is the Ricci scalar, and $G_{\mu\nu}$ is the Einstein tensor. The above Lagrangian was first derived by Horndeski in a different form Ref. [32]. This Lagrangian (Eqs. (8)–(12)) is equivalent to that derived by Horndeski [35]. The total action is then given by

$$S = \int d^4x\sqrt{-g}(\mathcal{L} + \mathcal{L}_m), \tag{13}$$

where g represents a determinant of the metric $g_{\mu\nu}$, and $\mathcal{L}_m$ is the Lagrangian of non-relativistic matter.

Variation with respect to the metric produces the gravity equations, and variation with respect to the scalar field ϕ yields the equation of motion. By using the notation $K \equiv K(\phi,X)$, $G \equiv G_3(\phi,X)$, $F \equiv \frac{2}{M_{\rm pl}^2}G_4(\phi,X)$, and assuming $G_5(\phi,X) = 0$ for Friedmann–Robertson–Walker spacetime, the gravity equations give

$$3M_{\rm pl}^2FH^2 = \rho_m + \rho_r - 3M_{\rm pl}^2H\dot{F} - K + 2XK_{,X} + 6H\dot{\phi}XG_{,X} - 2XG_{,\phi}, \tag{14}$$

$$-M_{\rm pl}^2F(3H^2 + 2\dot{H}) = p_r + 2M_{\rm pl}^2H\dot{F} + M_{\rm pl}^2\ddot{F} + K - 2XG_{,X}\ddot{\phi} - 2XG_{,\phi}, \tag{15}$$

and the equation of motion for the scalar field gives

$$\begin{aligned}&(K_{,X} + 2XK_{,XX} + 6H\dot{\phi}G_{,X} + 6H\dot{\phi}XG_{,XX} - 2XG_{,\phi X} - 2G_{,\phi})\ddot{\phi} \\ &+(3HK_{,X} + \dot{\phi}K_{,\phi X} + 9H^2\dot{\phi}G_{,X} + 3\dot{H}\dot{\phi}G_{,X} + 6HXG_{,\phi X} - 6HG_{,\phi} - G_{,\phi\phi}\dot{\phi})\dot{\phi} \\ &-K_{,\phi} - 6M_{\rm pl}^2H^2F_{,\phi} - 3M_{\rm pl}^2\dot{H}F_{,\phi} = 0.\end{aligned} \tag{16}$$

Here, an overdot denotes differentiation with respect to cosmic time t, and $H = \dot{a}/a$ is the Hubble expansion rate. Note that we use the partial derivative notation $K_{,X} \equiv \partial K/\partial X$ and

$K_{,XX} \equiv \partial^2 K/\partial X^2$ and a similar notation for other variables. Also, ρ_m and ρ_r are the energy densities of matter and radiation, respectively, and p_r is the pressure of the radiation.

In the kinetic gravity braiding model [30], the functions in Horndeski's theory are given as follows:

$$K(\phi,X) = -X, \tag{17}$$

$$G_3(\phi,X) = M_{\rm pl}\left(\frac{r_c^2}{M_{\rm pl}^2}X\right)^n, \tag{18}$$

$$G_4(\phi,X) = \frac{M_{\rm pl}^2}{2}, \tag{19}$$

$$G_5(\phi,X) = 0. \tag{20}$$

$M_{\rm pl}$ is the reduced Planck mass related to Newton's gravitational constant by $M_{\rm pl} = 1/\sqrt{8\pi G}$, and r_c is called the crossover scale in the DGP model [42]. The kinetic braiding model we study is characterized by parameter n in Eq. (18). For n = 1, this corresponds to Deffayet's Galileon cosmological model [22]. For n equal to infinity, the background expansion of the universe of the kinetic braiding model approaches that of the ΛCDM model. This helps distinguish the kinetic braiding model from the ΛCDM model.

In the case of the kinetic braiding model using the Hubble parameter as the present epoch H_0, the crossover scale r_c is given by

$$r_c = \left(\frac{2^{n-1}}{3n}\right)^{1/2n}\left[\frac{1}{6(1-\Omega_{m,0}-\Omega_{r,0})}\right]^{(2n-1)/4n} H_0^{-1}, \tag{21}$$

where $\Omega_{r,0}$ is the density parameter of the radiation at the present time. Thus, the independent parameters of the cosmological model are n and $\Omega_{m,0}$. The effective gravitational constant normalized to Newton's gravitational constant $G_{\rm eff}$ / G of the kinetic braiding model is given by

$$\frac{G_{\rm eff}}{G} = \frac{2n+3n\Omega_m-\Omega_m}{\Omega_m(5n-\Omega_m)}, \tag{22}$$

where Ω_m is the matter energy density parameter defined as $\Omega_m = \rho_m/3M_{\rm pl}^2H^2$. Here, we used the attractor condition. Although the background evolution for large n approaches the ΛCDM model, the growth history of matter density perturbations is different due to the time-dependent effective gravitational constant.

2.3. Galileon model

The Galileon gravity model is proposed as an alternative to the dark energy model. It is thought that the Galileon model studied in Refs. [16, 17] is a specific aspect of Horndeski's theory [32].

In the Galileon model [16, 17], the functions in the Lagrangian (Eqs. (8)–(12)) of the Horndeski's theory are given as follows:

$$K(\phi,X) = 2\frac{\omega}{\phi}X, \tag{23}$$

$$G_3(\phi,X) = 2\xi(\phi)X, \tag{24}$$

$$G_4(\phi,X) = \phi, \tag{25}$$

$$G_5(\phi,X) = 0, \tag{26}$$

where ω is the Brans–Dicke parameter and $\xi(\phi)$ is a function of ϕ.

In this case, the Friedmann-like equations, Eqs. (14) and (15), can be written in the following forms, respectively:

$$3H^2 = \frac{1}{M_{\rm pl}^2}(\rho_m + \rho_r + \rho_\phi), \tag{27}$$

$$-3H^2 - 2\dot{H} = \frac{1}{M_{\rm pl}^2}(p_r + p_\phi), \tag{28}$$

where the effective dark energy density ρ_ϕ is defined as

$$\rho_\phi = 2\phi\left[-3H\frac{\dot{\phi}}{\phi} + \frac{\omega}{2}\left(\frac{\dot{\phi}}{\phi}\right)^2 + \phi^2\xi(\phi)\left\{3H + \frac{\dot{\phi}}{\phi}\right\}\left(\frac{\dot{\phi}}{\phi}\right)^3\right] + 3H^2(M_{\rm pl}^2 - 2\phi), \tag{29}$$

and the effective pressure of dark energy p_ϕ is

$$p_\phi = 2\phi\left[\frac{\ddot{\phi}}{\phi} + 2H\frac{\dot{\phi}}{\phi} + \frac{\omega}{2}\left(\frac{\dot{\phi}}{\phi}\right)^2 - \phi^2\xi(\phi)\left\{\frac{\ddot{\phi}}{\phi} - \left(\frac{\dot{\phi}}{\phi}\right)^2\right\}\left(\frac{\dot{\phi}}{\phi}\right)^2\right] - (3H^2 + 2\dot{H})(M_{\rm pl}^2 - 2\phi). \tag{30}$$

The equation of motion for the scalar field is given by Eq. (16).

For the numerical analysis, we adopt a specific model in which

$$\xi(\phi) = \frac{r_c^2}{\phi^2}, \tag{31}$$

where r_c is the crossover scale [15]. This Galileon model extends the Brans–Dicke theory by adding the self-interaction term, $\xi(\phi)(\nabla\phi)^2\Box\phi$. Thus, ω of this model is not exactly the same as the original Brans–Dicke parameter. The evolution of matter density perturbations of this model was computed in Refs. [16, 17].

At early times, we set the initial condition $\phi \simeq M_{\rm pl}^2/2$ to recover general relativity. Using these initial conditions reduces the Friedmann equations (Eqs. (27) and (28)) to their usual forms: $3H^2 = (\rho_m + \rho_r)/M_{\rm pl}^2$ and $-3H^2 - 2\dot{H} = p_r/M_{\rm pl}^2$. This is the cosmological version of the Vainshtein effect [23], which is a method to recover general relativity below a certain scale. At present, to induce cosmic acceleration, the value of r_c must be fine tuned.

The energy density parameter of matter at present in this model is defined as $\Omega_{m,0} = \rho_{m,0}/3H_0^2\phi_0$. Therefore, in the numerical analysis, the value of r_c is fine tuned so that $\Omega_{m,0}$ becomes an assumed value. Thus, the independent parameters of the cosmological model are ω and $\Omega_{m,0}$. For the Galileon model specified by Eqs. (23)–(26) and (31), the effective gravitational constant is given by

$$G_{\rm eff} = \frac{1}{16\pi\phi}\left[1 + \frac{(1 + \xi(\phi)\dot{\phi}^2)^2}{J}\right], \tag{32}$$

where

$$J \equiv 3 + 2\omega + \phi^2\xi(\phi)\left[4\frac{\ddot{\phi}}{\phi} - 2\frac{\dot{\phi}^2}{\phi^2} + 8H\frac{\dot{\phi}}{\phi} - \phi^2\xi(\phi)\frac{\dot{\phi}^4}{\phi^4}\right]. \tag{33}$$

The effective gravitational constant $G_{\rm eff}$ is close to Newton's constant G at early times, but increases at later times.

3. Cosmic growth rate

3.1. Density perturbations

Under the quasistatic approximation on sub-horizon scales, the evolution equation for cold dark matter over-density δ in linear theory is given by

$$\ddot{\delta} + 2H\dot{\delta} - 4\pi G_{\rm eff}\rho\delta \simeq 0, \tag{34}$$

where $G_{\rm eff}$ represents the effective gravitational constant of the modified gravity models described in the previous section.

We set the same initial conditions as in the conventional ΛCDM case ($\delta \approx a$ and $\dot{\delta} \approx \dot{a}$) because we trace the difference between the evolution of the matter perturbations in modified gravity and the evolution in the ΛCDM model. From the evolution equation, we numerically obtain the growth factor δ / a for modified gravity models. The linear growth rate is written as

$$f = \frac{d\ \ln\delta}{d\ \ln a}. \tag{35}$$

where δ is the matter density fluctuations and a is the scale factor. The growth rate can be parameterized by the growth index γ, defined by

$$f = \Omega_m^{\gamma}. \tag{36}$$

Refs. [48, 49] showed that the growth rate f in the Galileon model specified by Eqs. (23)–(26) and (31) is enhanced compared with the ΛCDM model for the same value of $\Omega_{m,0}$ due to enhancement of the effective gravitational constant.

3.2. Euclid

Euclid [39] is a European Space Agency mission that is prepared for a launch at the end of 2020. The aim of Euclid is to study the origin of the accelerated expansion of the universe. Euclid will investigate the distance-redshift relationship and the evolution of cosmic structures by measuring shapes and redshifts of galaxies and the distribution of clusters of galaxies over a large part of the sky. Its main subject of research is the nature of dark energy. However, Euclid will cover topics including cosmology, galaxy evolution, and planetary research.

In this study, Euclid parameters are adopted as the growth rate observations. The growth rate can be parameterized by using the growth index γ, defined by $f = \Omega_m{}^{\gamma}$. Mock data of the cosmic growth rate are built based on the 1σ marginalized errors of the growth rate by Euclid. These data are listed in Table 4 in the paper by Amendola et al. [39]. **Table 1** shows the 1σ marginalized errors for the cosmic growth rates with respect to each redshift in accordance with Table 4 in [39]. In **Figure 1**, the mock data of the cosmic growth rate used in this study are plotted.

The mock data are used to compute the statistical χ^2 function. The χ^2 function for the growth rate is defined as

$$\chi_f^2 = \sum_{i=1}^{14} \frac{\left(f_{theory}(z_i) - f_{obs}(z_i)\right)^2}{\sigma_{f_g}(z_i)^2} \tag{37}$$

where $f_{obs}(z_i)$ is the future observational (mock) data of the growth rate. The theoretical growth rate $f_{theory}(z_i)$ is computed as Eq. (35). In Ref. [50], constraints on neutrino masses are estimated based on future observations of the growth rate of the cosmic structure from the Euclid redshift survey.

The estimated errors from the observational technology of Euclid are known, but the center value of future observations is not known. Therefore, the purpose of this study is not to validate the ΛCDM model or modified gravity but to find ways and probabilities to distinguish between the ΛCDM model and modified gravity.

Experiment	z	σ_{f_g} (ref.)
Euclid [39]	0.7	0.011
	0.8	0.010
	0.9	0.009
	1.0	0.009
	1.1	0.009
	1.2	0.009
	1.3	0.010
	1.4	0.010
	1.5	0.011
	1.6	0.012
	1.7	0.014
	1.8	0.014
	1.9	0.017
	2.0	0.023

Here, z represents the redshift and σ_{f_g} represents the 1σ marginalized errors of the growth rates.

Table 1. 1σ marginalized errors for the growth rates in each redshift bin based on Table 4 in the study by Amendola et al. [39].

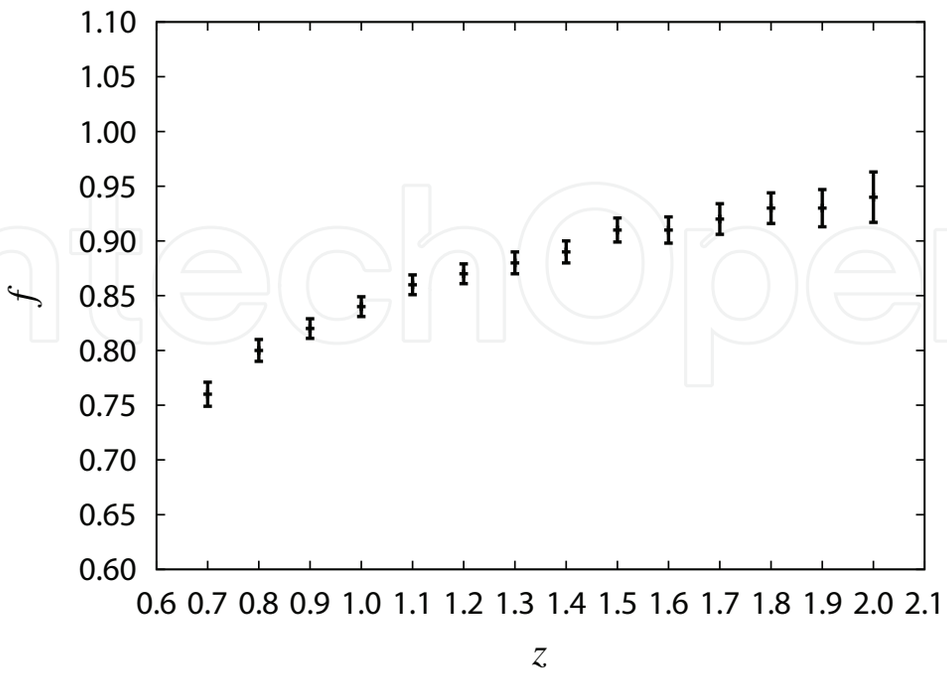

Figure 1. Plot of mock data of the cosmic growth rate.

http://dx.doi.org/10.5772/intechopen.68281

4. Comparison with observations

4.1. Extended DGP model

In **Figure 2**, we plot the probability contours in the (α, σ_8)-plane in the extended DGP model from the observational (mock) data of the cosmic growth rate by Euclid. The blue (dark) and light blue (light) contours show the 1σ (68.3%) and 2σ (95.0%) confidence limits, respectively. Part of $\alpha = 0$ for the horizontal axis corresponds to the ΛCDM model, and part of $\alpha = 1$ corresponds to the original DGP model. σ_8 is the root mean square (rms) amplitude of over-density at the comoving $8\,h^{-1}$ Mpc scale (where h is the normalized Hubble parameter $H_0 = 100\,h\mathrm{kmsec}^{-1}\mathrm{Mpc}^{-1}$). In **Figures 3–5**, we demonstrate why σ_8 is stringently constrained.

We plot $f\sigma_8$ (the product of growth rate and σ_8) in the extended DGP model as a function of redshift z for various values of the energy density parameter of matter at the present $\Omega_{m,0}$ in **Figures 3–5**. In **Figure 3**, the parameters are fixed by α = 1, σ_8 = 0.6. For the various values of $\Omega_{m,0}$, the theoretical curves seem to revolve around the dashed circle. Hence, the value of σ_8 = 0.6 is incompatible with the observational (mock) data.

In **Figure 4**, the parameters are fixed by α = 1, σ_8 = 1.0. For the various values of $\Omega_{m,0}$, the theoretical curves seem to revolve around the dashed circle. Hence, the value of σ_8 = 1.0 is incompatible with the observational (mock) data.

In **Figure 5**, the parameters are fixed by α = 1, σ_8 = 0.855. For the various values of $\Omega_{m,0}$, although the theoretical curves seem to revolve around the dashed circle, some theoretical curves are comparatively close to the observational (mock) data. Hence, the value of σ_8 = 0.855 is compatible with the observational (mock) data in the original DGP model (α = 1).

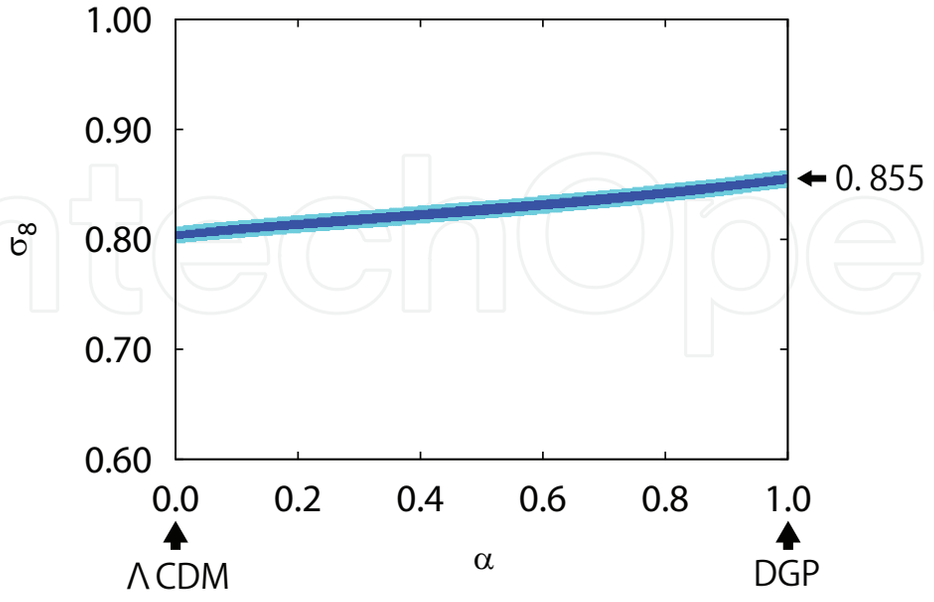

Figure 2. Probability contours in the (α, σ_8)-plane for the extended DGP model from the observational (mock) data of the cosmic growth rate by Euclid. The contours show the 1σ (68.3%) and 2σ (95.0%) confidence limits.

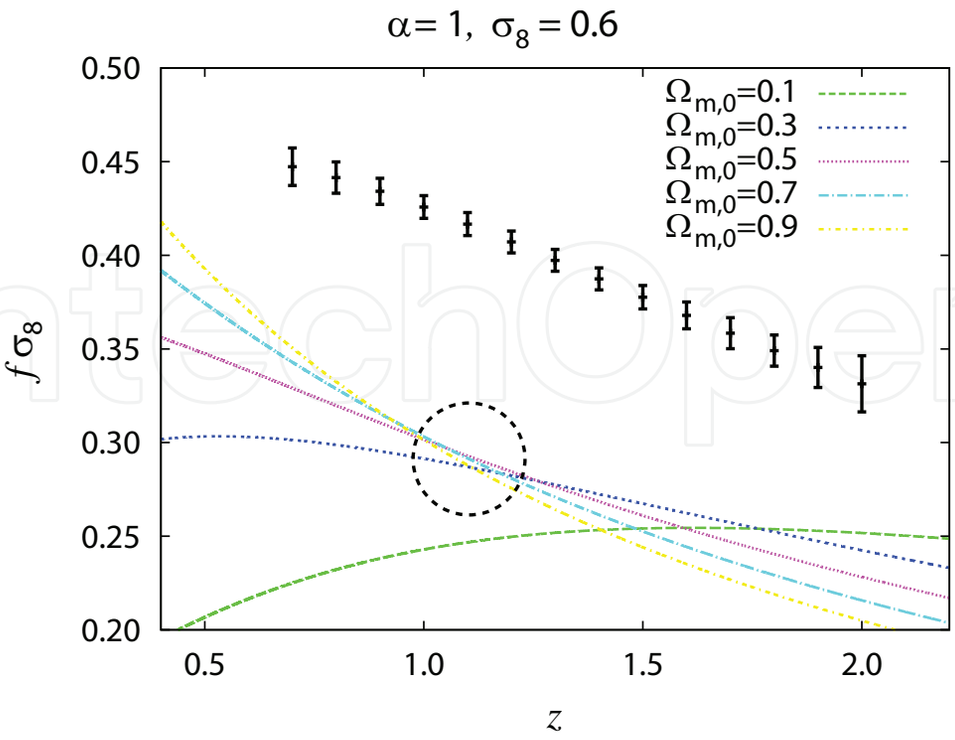

Figure 3. $f\sigma_8$ (the product of growth rate and σ_8) in the extended DGP model as a function of redshift z for various values of $\Omega_{m,0}$. The parameters are fixed by $\alpha = 1$, $\sigma_8 = 0.6$.

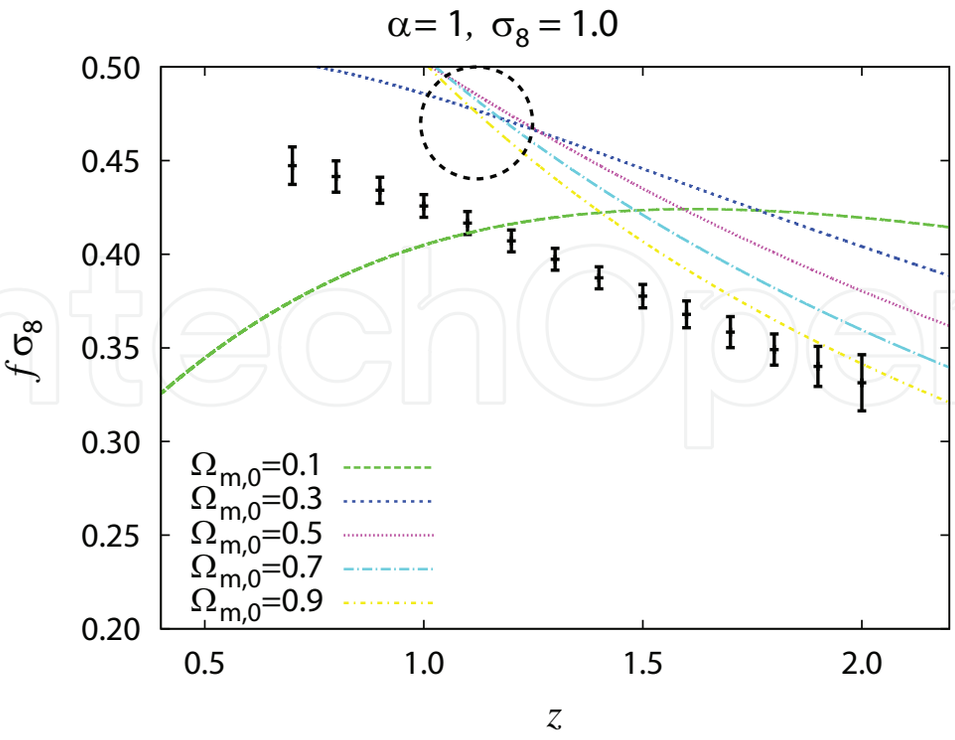

Figure 4. $f\sigma_8$ in the extended DGP model as a function of redshift z for various values of $\Omega_{m,0}$. The parameters are fixed by $\alpha = 1$, $\sigma_8 = 1.0$.

http://dx.doi.org/10.5772/intechopen.68281

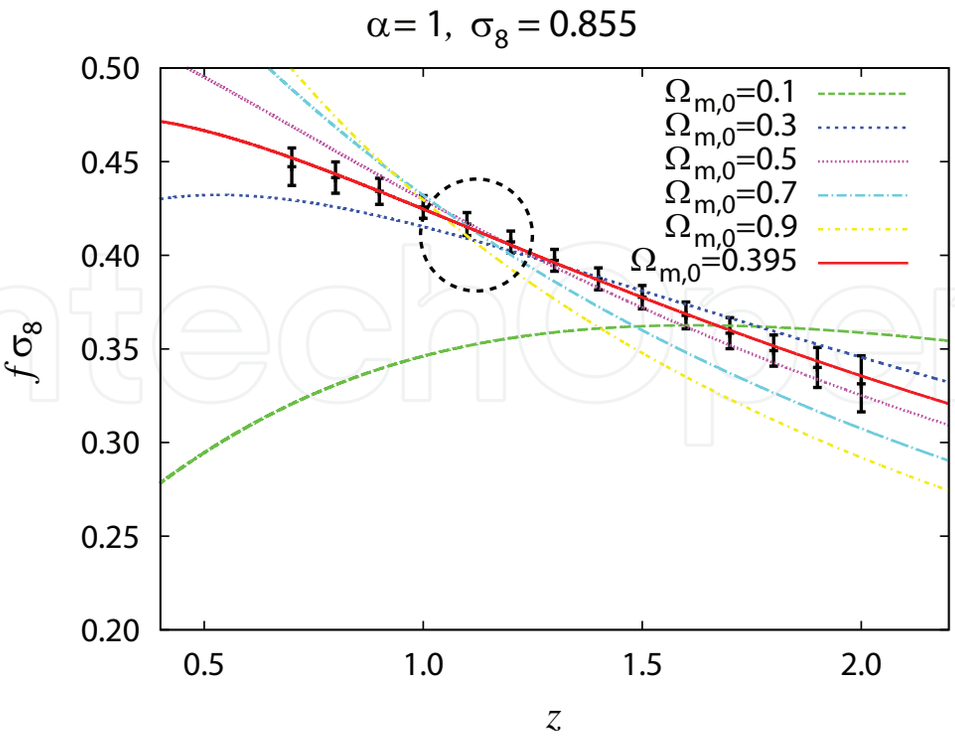

Figure 5. $f\sigma_8$ in the extended DGP model as a function of redshift z for various values of $\Omega_{m,0}$. The parameters are fixed by $\alpha = 1$, $\sigma_8 = 0.855$.

In **Figure 6**, we plot the probability contours in the (α, $\Omega_{m,0}$)-plane in the extended DGP model from the observational (mock) data of the cosmic growth rate by Euclid. The red (dark) and pink (light) contours show the 1σ (68.3%) and 2σ (95.0%) confidence limits, respectively. We demonstrate why $\Omega_{m,0}$ is positively correlated with α in **Figure 7**.

We plot $f\sigma_8$ in the extended DGP model as a function of redshift z in **Figure 7**. The red (solid) line is the theoretical curve for the best-fit parameter in the ΛCDM model ($\alpha = 0$, $\Omega_{m,0} = 0.257$, $\sigma_8 = 0.803$). In the case of changing only α =1, the growth rate $f\sigma_8$ is suppressed due to suppression of the effective gravitational constant (green (dashed) line: $\alpha = 1$, $\Omega_{m,0} = 0.257$, $\sigma_8 = 0.803$). For $\alpha = 1$, by tuning the value of $\Omega_{m,0}$ and σ_8, the theoretical curve is compatible with the observational (mock) data again (blue (dotted) line: $\alpha = 1$, $\Omega_{m,0} = 0.395$, $\sigma_8 = 0.855$).

In **Figure 8**, we add constraints on $\Omega_{m,0}$ for the extended DGP model from the combination of CMB, BAO, and SNIa data (black solid lines) [46] to the probability contours in the (α, $\Omega_{m,0}$)-plane by the growth rate (mock) data by Euclid of **Figure 6**.

Because $\Omega_{m,0}$ is stringently constrained by the cosmic growth rate data from Euclid, we find the ΛCDM model is distinguishable from the original DGP model by combining the growth rate data of Euclid with other observations.

4.2. Kinetic gravity braiding model

In **Figure 9**, we plot the probability contours in the (n, $\Omega_{m,0}$)-plane in the kinetic gravity braiding model from the observational (mock) data of the cosmic growth rate by Euclid. The red (dark) and pink (light) contours show the 1σ (68.3%) and 2σ (95.0%) confidence limits, respectively.

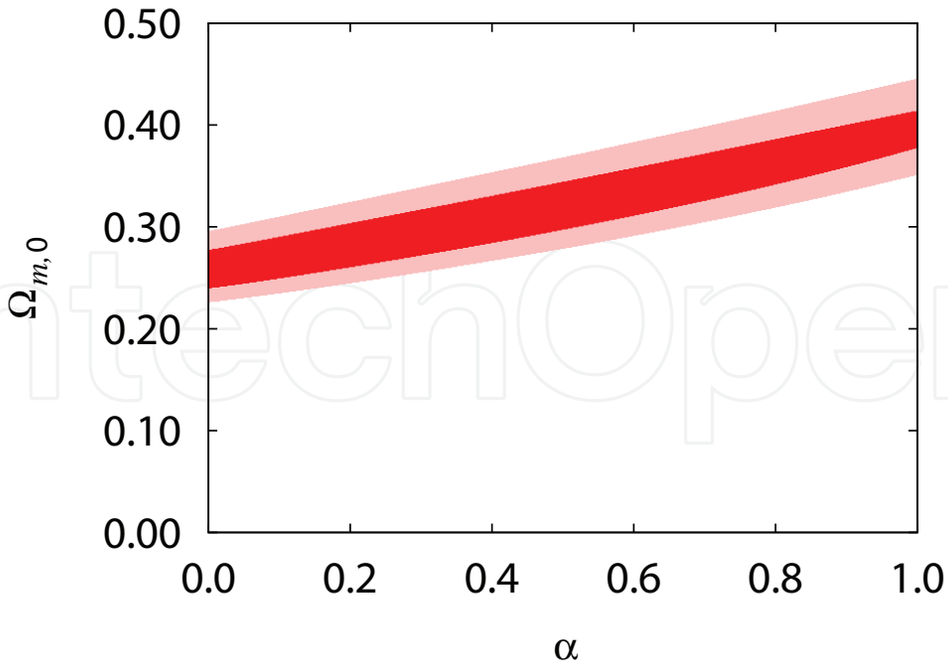

Figure 6. Probability contours in the (α, $\Omega_{m,0}$)-plane for the extended DGP model from the observational (mock) data of the cosmic growth rate by Euclid. The contours show the 1σ (68.3%) and 2σ (95.0%) confidence limits.

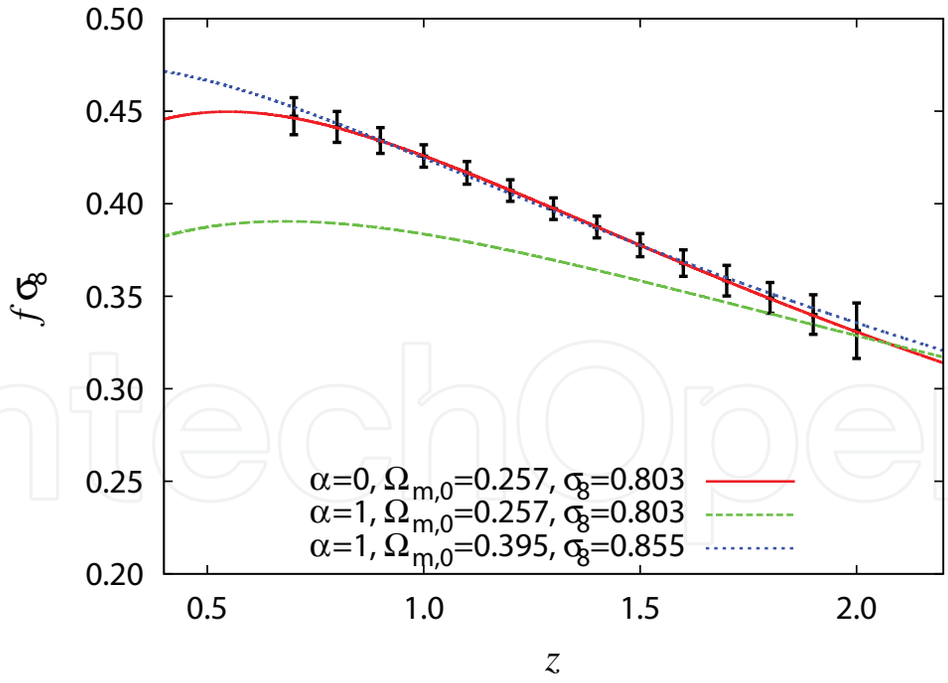

Figure 7. $f\sigma_8$ in the extended DGP model as a function of redshift z. The values of the parameters are as follows. Red (solid) line: $\alpha = 0$, $\Omega_{m,0} = 0.257$, $\sigma_8 = 0.803$. Green (dashed) line: $\alpha = 1$, $\Omega_{m,0} = 0.257$, $\sigma_8 = 0.803$. Blue (dotted) line: $\alpha = 1$, $\Omega_{m,0} = 0.395$, $\sigma_8 = 0.855$.

http://dx.doi.org/10.5772/intechopen.68281

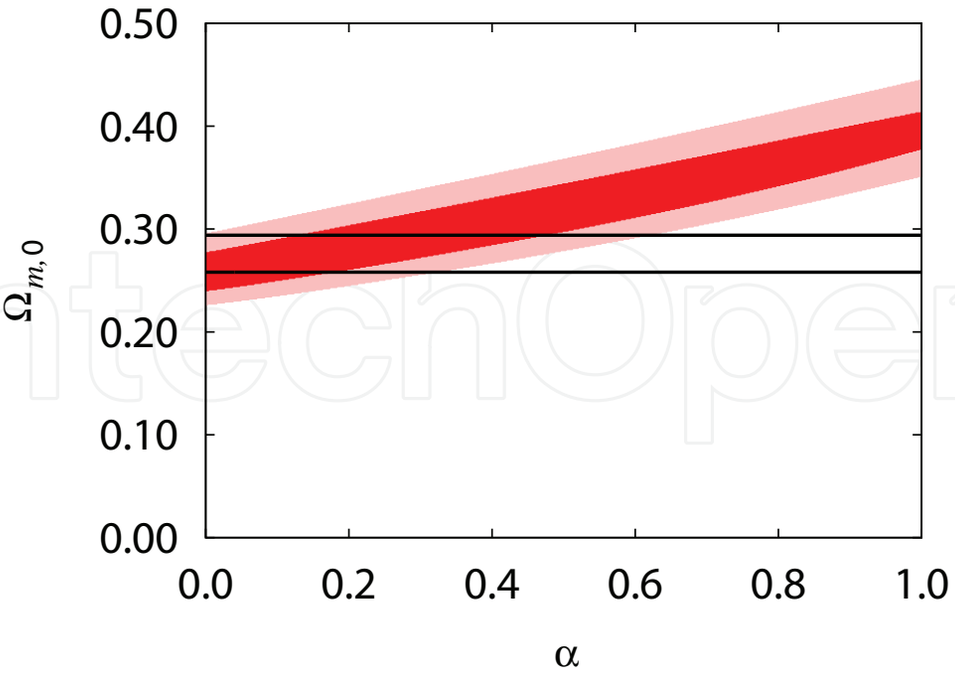

Figure 8. Addition of constraints on $\Omega_{m,0}$ for the extended DGP model from CMB, BAO and SNIa data [46] to the data in **Figure 6**.

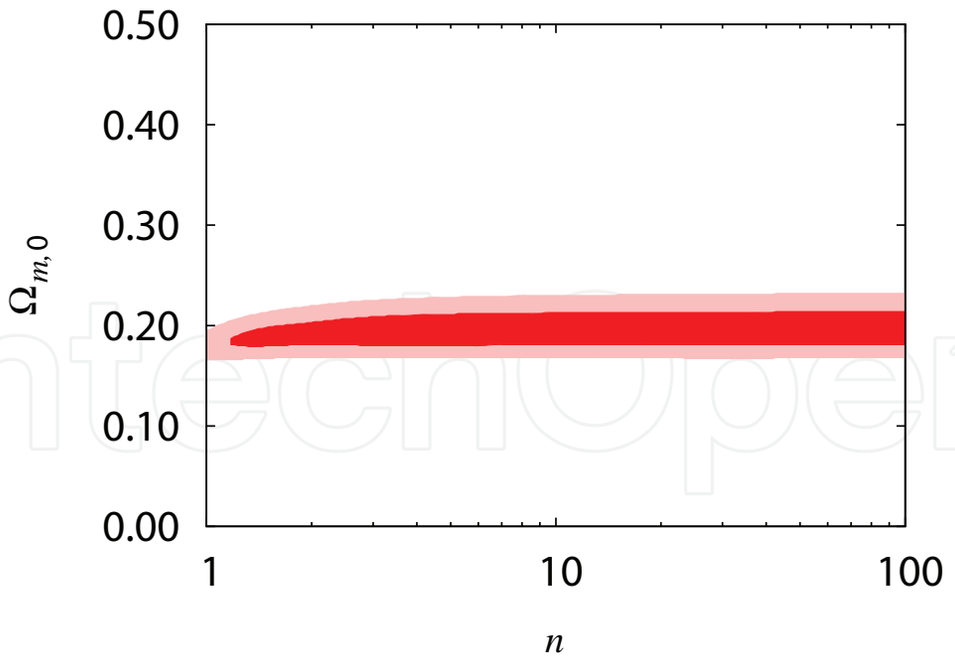

Figure 9. Probability contours in the (n, $\Omega_{m,0}$)-plane for the kinetic gravity braiding model from the observational (mock) data of the cosmic growth rate by Euclid. The contours show the 1σ (68.3%) and 2σ (95.0%) confidence limits.

We plot $f\sigma_8$ in the kinetic gravity braiding model as a function of redshift z in **Figure 10**. The red (solid) line is the theoretical curve for the best-fit parameter in the ΛCDM model ($\Omega_{m,0} = 0.257$, $\sigma_8 = 0.803$). In the case of the kinetic gravity braiding model for $n = 1$, the growth rate $f\sigma_8$ is enhanced due to enhancement of the effective gravitational constant (Green (dashed) line: $n = 1$, $\Omega_{m,0} = 0.257$, $\sigma_8 = 0.803$). For $n = 100$, by tuning the value of $\Omega_{m,0}$ and σ_8, the theoretical curve is compatible with the observational (mock) data again (blue (dotted) line: $n = 100$, $\Omega_{m,0} = 0.196$, $\sigma_8 = 0.820$).

In **Figure 11**, we add constraints on $\Omega_{m,0}$ for the kinetic gravity braiding model from CMB (black dashed lines) and from SNIa (black solid lines) [30], respectively, to the probability contours in the (n, $\Omega_{m,0}$)-plane by the growth rate (mock) data by Euclid of **Figure 9**.

In the kinetic gravity braiding model, the allowed parameter region obtained by using only the growth rate data does not overlap with the allowed parameter region obtained from CMB or from SNIa data.

4.3. Galileon model

In **Figure 12**, we plot the probability contours in the (ω, $\Omega_{m,0}$)-plane in the Galileon model from the observational (mock) data of the cosmic growth rate by Euclid. The red (dark) and pink (light) contours show the 1σ (68.3%) and 2σ (95.0%) confidence limits, respectively. We also plot the constraints on $\Omega_{m,0}$ for the Galileon model from the combination of CMB, BAO, and SNIa (black solid lines) [49].

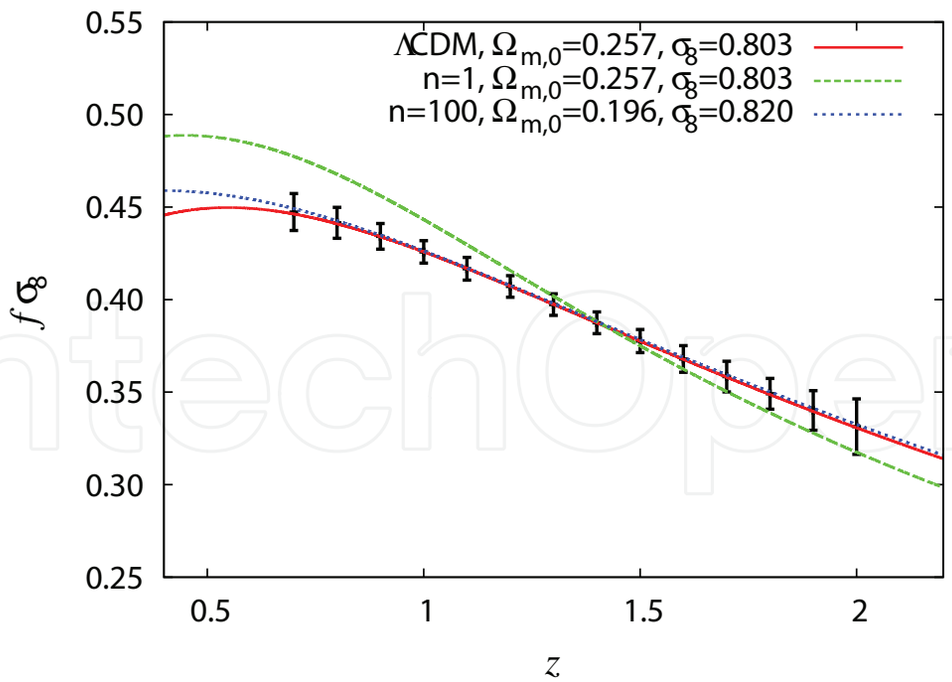

Figure 10. $f\sigma_8$ in kinetic gravity braiding model as a function of redshift z. The values of the parameters are as follows. Red (solid) line: ΛCDM, $\Omega_{m,0} = 0.257$, $\sigma_8 = 0.803$. Green (dashed) line: $n = 1$, $\Omega_{m,0} = 0.257$, $\sigma_8 = 0.803$. Blue (dotted) line: $n = 100$, $\Omega_{m,0} = 0.196$, $\sigma_8 = 0.820$.

http://dx.doi.org/10.5772/intechopen.68281

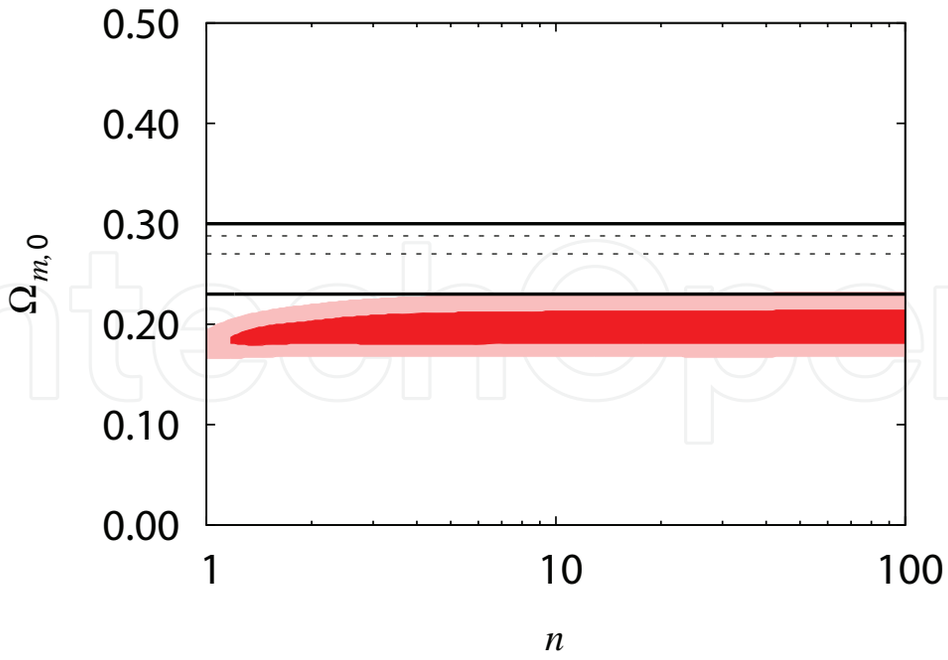

Figure 11. Addition of constraints on $\Omega_{m,0}$ for the kinetic gravity braiding model from CMB (black dashed lines) and from SNIa (black solid lines), respectively, [30] to **Figure 9**.

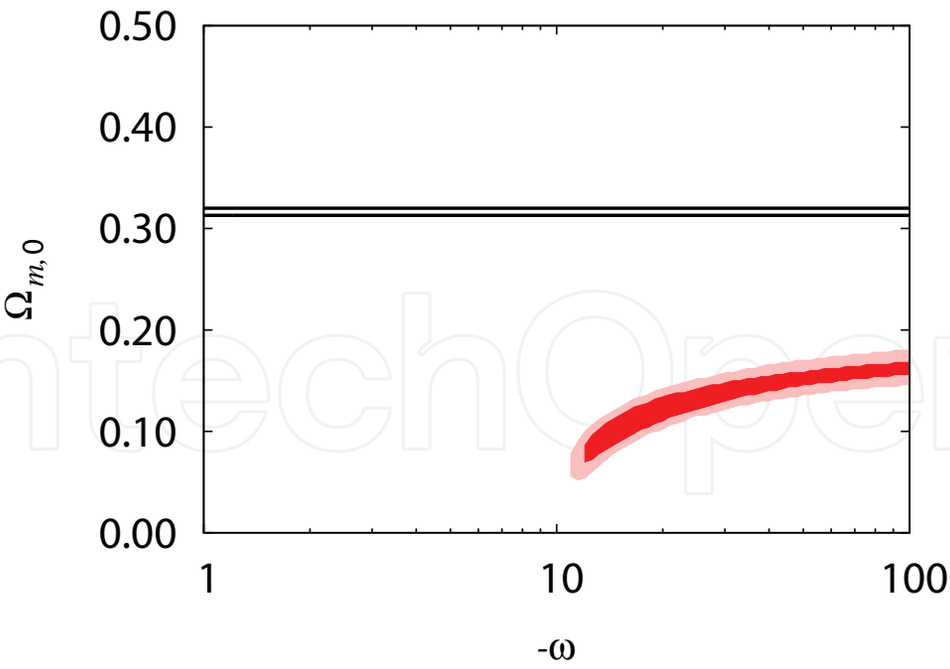

Figure 12. Probability contours in the (ω, $\Omega_{m,0}$)-plane for the Galileon model from the observational (mock) data of the cosmic growth rate by Euclid. The contours show the 1σ (68.3%) and 2σ (95.0%) confidence limits. The added constraints on $\Omega_{m,0}$ for the Galileon model are from the combination of CMB, BAO, and SNIa (black solid lines) [49].

In the Galileon model, the allowed parameter region obtained by using only the growth rate data do not overlap at all with the allowed parameter region obtained from the combination of CMB, BAO, and SNIa data.

5. Conclusions

The growth rate $f\sigma_8$ in the original DGP model is suppressed in comparison with that in the ΛCDM case in the setting of the same value of $\Omega_{m,0}$ due to suppression of the effective gravitational constant. In the case of the kinetic gravity braiding model and the Galileon model, the growth rate $f\sigma_8$ is enhanced in comparison with the ΛCDM case in the same value of $\Omega_{m,0}$ due to enhancement of the effective gravitational constant. For the cosmic growth rate data from the future observation, compatible values of $\Omega_{m,0}$ differ according to the model. Furthermore, values of $\Omega_{m,0}$ can be stringently constrained. Thus, we find the ΛCDM model is distinguishable from modified gravity by combining the growth rate data of Euclid with other observations.

The estimated errors from the observational technology of Euclid are known, but the center value of future observations is not known. If the center value of the cosmic growth rate of future observations is different from that of this chapter, the valid model can differ from that of this chapter. However, the methods in this chapter are useful for distinguishing between the ΛCDM model and modified gravity.

In this chapter, assuming the function $G_5(\phi, X)$ in Horndeski's theory $G_5(\phi, X) = 0$, we compute the linear matter density perturbations for the growth rate. In future work, we will study the model having non-zero function $G_5(\phi, X)$ in Horndeski's theory and investigate the nonlinear effect.

Acknowledgements

This work was supported by a Grant-in-Aid for Scientific Research from the Japan Society for the Promotion of Science (Grant Number 25400264).

Author details

Koichi Hirano

Address all correspondence to: k_hirano@tsuru.ac.jp

Department of Primary Education, Tsuru University, Yamanashi, Japan

References

[1] Riess AG, et al. Observational evidence from supernovae for an accelerating universe and a cosmological constant. The Astronomical Journal. 1998;**116**:1009–1038. DOI: 10.1086/300499

[2] Perlmutter S, et al. Measurements of Ω and Λ from 42 high-redshift supernovae. The Astrophysical Journal. 1999;**517**:565–586. DOI: 10.1086/307221

[3] Ratra B, Peebles PJE. Cosmological consequences of a rolling homogeneous scalar field. Physical Review D. 1988;**37**:3406–3427. DOI: 10.1103/PhysRevD.37.3406

[4] Caldwell RR. A phantom menace? Cosmological consequences of a dark energy component with super-negative equation of state. Physics Letters B. 2002;**545**:23–29. DOI: 10.1016/S0370-2693(02)02589-3

[5] Komiya Z, Kawabata K, Hirano K, Bunya H, Yamamoto N. Galaxy merging and number vs. apparent magnitude relation for the universe with a time-decaying cosmological term. Astronomy & Astrophysics. 2006;**449**:903–916. DOI: 10.1051/0004-6361:20054406

[6] Komiya Z, Kawabata K, Hirano K, Bunya H, Yamamoto N. Constraints on Λ-decaying cosmology from observational point of view. Journal of Korean Astronomical Society. 2005;**38**:157–160. DOI: 10.5303/JKAS.2005.38.2.157

[7] De Felice A, Tsujikawa S. f(R) Theories. Living Reviews in Relativity. 2010;**13**:3. DOI: 10.12942/lrr-2010-3

[8] Hirano K, Komiya Z. Observational tests for oscillating expansion rate of the Universe. Physical Review D. 2010;**82**:103513. DOI: 10.1103/PhysRevD.82.103513

[9] Hirano K, Kawabata K, Komiya Z. Spatial periodicity of galaxy number counts, CMB anisotropy, and SNIa Hubble diagram based on the universe accompanied by a non-minimally coupled scalar field. Astrophysics and Space Science. 2008;**315**:53–72. DOI: 10.1007/s10509-008-9794-7

[10] Hartnett JG, Hirano K. Galaxy redshift abundance periodicity from Fourier analysis of number counts N(z) using SDSS and 2dF GRS galaxy surveys. Astrophysics and Space Science. 2008;**318**:13–24. DOI: 10.1007/s10509-008-9906-4

[11] Dvali G, Gabadadze G, Porrati M. 4D gravity on a brane in 5D Minkowski space. Physics Letters B. 2000;**485**:208–214. DOI: 10.1016/S0370-2693(00)00669-9

[12] Hirano K, Komiya Z. Crossing the phantom divide in extended Dvali-Gabadadze-Porrati gravity. General Relativity and Gravitation. 2010;**42**:2751–2763. DOI: 10.1007/s10714-010-1030-4

[13] Hirano K, Komiya Z. Observational constraints on phantom crossing DGP gravity. International Journal of Modern Physics. 2011;**D20**:1–16. DOI: 10.1142/S0218271811018585

[14] Nicolis A, Rattazzi R, Trincherini E. Galileon as a local modification of gravity. Physical Review D. 2009;**79**:064036. DOI: 10.1103/PhysRevD.79.064036

[15] Chow N, Khoury J. Galileon cosmology. Physical Review D. 2009;**80**:024037. DOI: 10.1103/PhysRevD.80.024037

[16] Silva FP, Koyama K. Self-accelerating universe in Galileon cosmology. Physical Review D. 2009;**80**:121301. DOI: 10.1103/PhysRevD.80.121301

[17] Kobayashi T, Tashiro H, Suzuki D. Evolution of linear cosmological perturbations and its observational implications in Galileon-type modified gravity. Physical Review D. 2010;**81**:063513. DOI: 10.1103/PhysRevD.81.063513

[18] Kobayashi T. Cosmic expansion and growth histories in Galileon scalar-tensor models of dark energy. Physical Review D. 2010;**81**:103533. DOI: 10.1103/PhysRevD.81.103533

[19] Gannouji R, Sami M. Galileon gravity and its relevance to late time cosmic acceleration. Physical Review D. 2010;**82**:024011. DOI: 10.1103/PhysRevD.82.024011

[20] De Felice A, Tsujikawa S. Cosmology of a covariant Galileon field. Physical Review Letters. 2010;**105**:111301. DOI: 10.1103/PhysRevLett.105.111301

[21] De Felice A, Tsujikawa S. Generalized Galileon cosmology. Physical Review D. 2011;**84**: 124029. DOI: 10.1103/PhysRevD.84.124029

[22] Deffayet C, Pujolas O, Sawicki I, Vikman A. Imperfect dark energy from kinetic gravity braiding. Journal of Cosmology and Astroparticle Physics. 2010;**1010**:026. DOI: 10.1088/1475-7516/2010/10/026

[23] Vainshtein AI. To the problem of nonvanishing gravitation mass. Physics Letters B. 1972;**39**:393–394. DOI: 10.1016/0370-2693(72)90147-5

[24] Deffayet C, Esposito-Farese G, Vikman A. Covariant Galileon. Physical Review D. 2009;**79**:084003. DOI: 10.1103/PhysRevD.79.084003

[25] Deffayet C, Deser S, Esposito-Farese G. Generalized Galileons: All scalar models whose curved background extensions maintain second-order field equations and stress tensors. Physical Review D. 2009;**80**:064015. DOI: 10.1103/PhysRevD.80.064015

[26] Kobayashi T, Yamaguchi M, Yokoyama J. Inflation driven by the Galileon field. Physical Review Letters. 2010;**105**:231302. DOI: 10.1103/PhysRevLett.105.231302

[27] Mizuno S, Koyama K. Primordial non-Gaussianity from the DBI Galileons. Physical Review D. 2010;**82**:103518. DOI: 10.1103/PhysRevD.82.103518

[28] Kamada K, Kobayashi T, Yamaguchi M, Yokoyama J. Higgs G inflation. Physical Review D. 2011;**83**:083515. DOI: 10.1103/PhysRevD.83.083515

[29] Nesseris S, De Felice A, Tsujikawa S. Observational constraints on Galileon cosmology. Physical Review D. 2010;**82**:124054. DOI: 10.1103/PhysRevD.82.124054

[30] Kimura R, Yamamoto K. Large scale structures in the kinetic gravity braiding model that can be unbraided. Journal of Cosmology and Astroparticle Physics. 2011;**1104**:025. DOI: 10.1088/1475-7516/2011/04/025

[31] De Felice A, Kase R, Tsujikawa S. Matter perturbations in Galileon cosmology. Physical Review D. 2011;**83**:043515. DOI: 10.1103/PhysRevD.83.043515

[32] Horndeski GW. Second-order scalar-tensor field equations in a four-dimensional space. International Journal of Theoretical Physics. 1974;**10**:363–384. DOI: 10.1007/BF01807638

[33] Charmousis C, Copeland EJ, Padilla A, Saffin PM. General second-order scalar-tensor theory and self-tuning. Physical Review Letters. 2012;**108**:051101. DOI: 10.1103/PhysRevLett.108.051101

[34] Deffayet C, Gao X, Steer DA, Zahariade G. From k-essence to generalized Galileons. Physical Review D. 2011;**84**:064039. DOI: 10.1103/PhysRevD.84.064039

[35] Kobayashi T, Yamaguchi M, Yokoyama J. Generalized G-inflation: Inflation with the most general second-order field equations. Progress of Theoretical Physics. 2011;**126**:511–529. DOI: 10.1143/PTP.126.511

[36] Gleyzes J, Langlois D, Piazza F, Vernizzi F. New class of consistent scalar-tensor theories. Physical Review Letters. 2015;**114**:211101. DOI: 10.1103/PhysRevLett.114.211101

[37] Gleyzes J, Langlois D, Piazza F, Vernizzi F. Exploring gravitational theories beyond Horndeski. Journal of Cosmology and Astroparticle Physics. 2015;**1502**:018. DOI: 10.1088/1475-7516/2015/02/018

[38] Gao X. Unifying framework for scalar-tensor theories of gravity. Physical Review D. 2014;**90**:081501. DOI: 10.1103/PhysRevD.90.081501

[39] Amendola L, et al. Cosmology and fundamental physics with the Euclid satellite. Living Reviews in Relativity. 2013;**16**:6. DOI: 10.12942/lrr-2013-6

[40] Okada H, Totani T, Tsujikawa S. Constraints on f(R) theory and Galileons from the latest data of galaxy redshift surveys. Physical Review D. 2013;**87**:103002. DOI: 10.1103/PhysRevD.87.103002

[41] Dvali G, Turner MS. Dark energy as a modification of the Friedmann equation. 2003. arXiv:astro-ph/0301510

[42] Koyama K, Maartens R. Structure formation in the Dvali-Gabadadze-Porrati cosmological model. Journal of Cosmology and Astroparticle Physics. 2006;**0601**:016. DOI: 10.1088/1475-7516/2006/01/016

[43] Deffayet C. Cosmology on a brane in Minkowski bulk. Physics Letters B. 2001;**502**:199–208. DOI: 10.1016/S0370-2693(01)00160-5

[44] Deffayet C, Dvali G, Gabadadze G. Accelerated universe from gravity leaking to extra dimensions. Physical Review D. 2002;**65**:044023. DOI: 10.1103/PhysRevD.65.044023

[45] Koyama K. Ghosts in the self-accelerating universe. Classical and Quantum Gravity. 2007;**24**:R231–R253. DOI: 10.1088/0264-9381/24/24/R01

[46] Xia JQ. Constraining Dvali-Gabadadze-Porrati gravity from observational data. Physical Review D. 2009;**79**:103527. DOI: 10.1103/PhysRevD.79.103527

[47] De Felice A, Kobayashi T, Tsujikawa S. Effective gravitational couplings for cosmological perturbations in the most general scalar-tensor theories with second-order field equations. Physics Letters B. 2011;**706**:123–133. DOI: 10.1016/j.physletb.2011.11.028

[48] Hirano K. Observational tests of Galileon gravity with growth rate. General Relativity and Gravitation. 2016;**48**:138. DOI: 10.1007/s10714-016-2129-z

[49] Hirano K, Komiya Z, Shirai H. Constraining Galileon gravity from observational data with growth rate. Progress of Theoretical Physics. 2012;**127**:1041–1056. DOI: 10.1143/PTP.127.1041

[50] Hirano K. Neutrino masses from CMB B-mode polarization and cosmic growth rate. International Journal of Modern Physics. 2015;**A30**:1550001. DOI: 10.1142/S0217751X15500013